UDC 519.63

PFAFFIAN STRUCTURE AND SPECTRAL DYNAMICS OF A DISCRETE LOTKA–VOLTERRA OPERATOR: A FRAMEWORK FOR GEOLOGICAL EVIDENCE INTEGRATION

[1,2*]***Eshmamatova D.B.,*** [1]***Solijanova K.A.***

*24dil@mail.ru

[1]Tashkent State Transport University, Tashkent, Uzbekistan;

[2]V.I. Romanovskiy Institute of Mathematics, Uzbekistan Academy of Sciences, Tashkent, Uzbekistan

This paper investigates the connection between Pfaffian invariants, fixed-point geometry, and local spectral dynamics of a discrete Lotka–Volterra operator on the four-dimensional simplex. For an interaction tournament containing four cyclic triples, the unique interior fixed points of the corresponding invariant two-dimensional faces form the vertices of a fixed-point card. Using an established orientation criterion and a specified sign convention, the cyclic configuration of this card is characterized by fourth-order principal Pfaffian invariants. Under positivity of the full Pfaffian vector, an interior fixed point is constructed explicitly through normalized Pfaffian ratios. The characteristic polynomial of the Jacobian at this point is expressed in terms of the interaction coefficients and the same invariants. The simplex tangent space is proved to be invariant under the Jacobian, and the restricted spectrum consists of two complex conjugate pairs with moduli greater than one, establishing locally repelling dynamics with oscillatory components. These results place fixed-point geometry and local spectral behavior within a common algebraic framework, providing explicit formulas suitable for computational analysis. A mathematical interpretation for integrating five groups of geological evidence is also proposed. Distances to fixed-point configurations and interaction-response measures are introduced as descriptors of evidence composition and interaction. Their potential use in gold prospectivity assessment requires calibration against exploration observations and independent empirical validation.

Keywords: discrete Lotka–Volterra operator, Pfaffian invariant, fixed-point card, interior fixed point, local spectrum, gold prospectivity assessment

Citation: Eshmamatova D.B., Solijanova K.A. 2026. Pfaffian structure and spectral dynamics of a discrete Lotka–Volterra operator: a framework for geological evidence integration. *Problems of Computational and Applied Mathematics.* 5(76): 95-118.

DOI: 10.71310/pcam.5_76.2026.07

1 Introduction

Discrete Lotka–Volterra operators constitute a fundamental class of nonlinear dynamical systems acting on finite-dimensional simplices [1]. They naturally arise in population dynamics, mathematical genetics, ecology, and evolutionary game theory, where the coordinates of a point of the simplex represent normalized frequencies or proportions of interacting entities. Beyond biological applications, the same formalism provides an effective mathematical framework for describing adaptive redistribution mechanisms in non-biological systems, including competing strategies, information sources, decision rules, and multi-agent interactions. The relationship between Volterra-type quadratic

stochastic operators, tournaments, fixed points, and Lyapunov functions was established in classical studies [2].

Recent work has also extended the study of Volterra operators to infinite-dimensional simplices, where Lyapunov functions provide tools for describing limiting behavior [3].

Let

$$S^{m-1} = \left\{ x = (x_1, \ldots, x_m) \in \mathbb{R}^m : x_i \geqslant 0, \quad \sum_{i=1}^{m} x_i = 1 \right\}$$

be the standard $(m-1)$-dimensional simplex. A discrete Lotka–Volterra operator on S^{m-1} is a mapping

$$V : S^{m-1} \to S^{m-1}$$

defined by

$$(Vx)_i = x_i \left(1 + \sum_{j=1}^{m} a_{ij} x_j \right), \qquad i = 1, \ldots, m, \tag{1}$$

where

$$A = (a_{ij})_{i,j=1}^{m}, \qquad a_{ij} = -a_{ji}, \qquad a_{ii} = 0.$$

The skew-symmetric matrix A is called the interaction matrix. The sign of a_{ij} determines the direction of dominance between the i-th and j-th components, while its absolute value measures the strength of the corresponding interaction.

A point $x^* \in S^{m-1}$ is called a fixed point of V if

$$Vx^* = x^*.$$

The set of all fixed points is denoted by $\mathrm{Fix}(V)$. If $x^* \in \operatorname{Int} S^{m-1}$, then $x_i^* > 0$ for all $i = 1, \ldots, m$. Therefore, the fixed point equation $Vx^* = x^*$ is equivalent to

$$Ax^* = 0, \qquad x_i^* > 0, \qquad \sum_{i=1}^{m} x_i^* = 1. \tag{2}$$

Thus, the existence of an interior fixed point is reduced to the existence of a positive normalized vector in the kernel of the skew-symmetric interaction matrix A. This observation shows that the local and global dynamics of the operator are strongly connected with the algebraic structure of A.

The sign pattern of A defines a tournament, that is, a complete oriented graph whose vertices correspond to the components of the system [4]. For each pair of vertices, exactly one directed edge is assigned according to the sign of the corresponding interaction coefficient. A triple of indices is called cyclic if the associated three directed edges form an oriented cycle. Such cyclic triples play a special role, since the restriction of the Lotka–Volterra operator to the corresponding two-dimensional invariant face has an interior fixed point on that face.

Volterra-type quadratic stochastic operators associated with homogeneous tournaments have also been investigated on finite-dimensional simplices [5].

Recent studies have also investigated Volterra-type operators associated with strange tournaments, with particular attention to interior fixed points and nonergodic behavior [6].

An important tool for describing the arrangement and interrelation of fixed points located on such invariant faces is the fixed-point card [7]. The vertices of the card correspond to fixed points on the relevant two-dimensional invariant faces, while the orientations of the edges connecting them are determined by the algebraic structure of the interaction

matrix, in particular by the signs of the corresponding Pfaffian invariants. In the case $m = 5$, the structure of the fixed-point card is closely related to the fourth-order principal Pfaffian invariants of the interaction matrix. In the nondegenerate case, the signs of these Pfaffians determine the orientations of the edges of the card. The fixed-point structure and spectral properties of a discrete Lotka–Volterra operator on the four-dimensional simplex were further studied in [8]. In contrast, the vanishing of a Pfaffian leads to a degenerate configuration, where a non-oriented edge and, in many cases, a continuum of fixed points may appear [9].

In continuous-time antisymmetric Lotka–Volterra systems, Pfaffian methods connect interaction-network topology with positive kernel vectors and coexistence properties [10]. Related studies of coupled cyclic interactions have examined connections between nonlinear dynamics and the structure of the linearized system [11].

The present paper is devoted to the cyclic configuration of the fixed-point card of a discrete Lotka–Volterra operator on the four-dimensional simplex S^4. We consider a class of operators whose associated tournament contains four cyclic triples. The corresponding equilibria on the cyclic two-dimensional faces generate a fixed-point card. Under a suitable sign convention, we show that when the relevant Pfaffian invariants are positive, this card forms a directed cycle. This cyclic configuration is not merely a combinatorial feature of the tournament; it is also directly related to the existence of an interior fixed point of the operator.

Building on established results on fixed-point cards and interior fixed-point existence, this paper develops an explicit connection between Pfaffian geometry and local spectral analysis for the four-cycle configuration considered here. The characteristic polynomial and the two oscillation frequencies are expressed through the interaction coefficients and the Pfaffian invariants that also determine the interior fixed point. Restricting the Jacobian to the invariant simplex tangent space separates the transverse unit eigenvalue from the dynamically relevant spectrum and establishes local repulsion. The resulting fixed-point configurations and interaction responses are further used to define descriptors for a proposed geological evidence-integration framework. This applied construction is presented as a mathematical formulation requiring subsequent calibration and empirical validation.

2 Algebraic Structure of the Operator: Interaction Matrix, Tournament and Pfaffian Invariants

In this section, we consider the discrete Lotka–Volterra operator on the four-dimensional simplex S^4 given by

$$V : \begin{cases} x_1' = x_1(1 - a_{12}x_2 - a_{13}x_3 - a_{14}x_4 + a_{15}x_5), \\ x_2' = x_2(1 + a_{12}x_1 - a_{23}x_3 - a_{24}x_4 + a_{25}x_5), \\ x_3' = x_3(1 + a_{13}x_1 + a_{23}x_2 - a_{34}x_4 - a_{35}x_5), \\ x_4' = x_4(1 + a_{14}x_1 + a_{24}x_2 + a_{34}x_3 - a_{45}x_5), \\ x_5' = x_5(1 - a_{15}x_1 - a_{25}x_2 + a_{35}x_3 + a_{45}x_4), \end{cases} \tag{3}$$

where

$$0 < a_{ij} \leqslant 1, \qquad 1 \leqslant i < j \leqslant 5.$$

The corresponding skew-symmetric interaction matrix is

$$A = \begin{pmatrix} 0 & -a_{12} & -a_{13} & -a_{14} & a_{15} \\ a_{12} & 0 & -a_{23} & -a_{24} & a_{25} \\ a_{13} & a_{23} & 0 & -a_{34} & -a_{35} \\ a_{14} & a_{24} & a_{34} & 0 & -a_{45} \\ -a_{15} & -a_{25} & a_{35} & a_{45} & 0 \end{pmatrix}, \tag{4}$$

so that $A^T = -A$. Here $a_{ij} \in (0, 1]$, $i < j$, are the parameters appearing in (3), and $A = (\alpha_{ij})$ denotes the signed interaction matrix given in (4).

The tournament corresponding to the operator is shown in Figure 1.

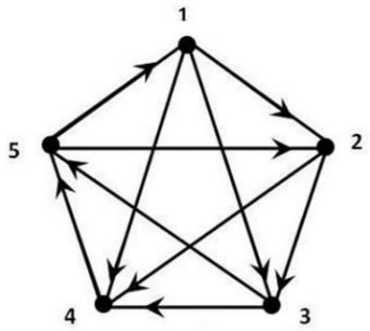


Figure 1 Tournament corresponding to the Lotka–Volterra operator.

From this tournament, the following cyclic triples are obtained:

$$(1, 3, 5), \qquad (1, 4, 5), \qquad (2, 3, 5), \qquad (2, 4, 5).$$

These cyclic triples determine the invariant two-dimensional faces whose interior fixed points will be used in the construction of the fixed-point card.

Since A is a skew-symmetric matrix of odd order [12],

$$\det A = 0.$$

Hence,

$$\operatorname{Ker} A \neq \{0\}.$$

For a 5×5 skew-symmetric matrix, a kernel vector can be expressed in terms of fourth-order Pfaffians. We introduce the following fourth-order principal Pfaffian invariants:

$$\Delta_1 = a_{23}a_{45} - a_{24}a_{35} - a_{25}a_{34},$$

$$\Delta_2 = a_{14}a_{35} - a_{13}a_{45} + a_{15}a_{34},$$

$$\Delta_3 = a_{12}a_{45} + a_{14}a_{25} - a_{15}a_{24},$$

$$\Delta_4 = a_{15}a_{23} - a_{12}a_{35} - a_{13}a_{25},$$

$$\Delta_5 = a_{12}a_{34} - a_{13}a_{24} + a_{14}a_{23}.$$

For convenience, the signs of the Pfaffian invariants are chosen here so that the directed cycle of the fixed-point card is characterized by positive inequalities. Accordingly, some of the Δ_i may differ by a sign from the corresponding Pfaffian quantities used in our previous notation. This is only a change of sign convention and does not alter the algebraic identities or the geometric fixed-point configuration.

With this convention, the cyclic orientation of the fixed-point card corresponds to

$$\Delta_i > 0, \qquad i = 1, 2, 3, 4.$$

Let $\boldsymbol{\Delta} = (\Delta_1, \Delta_2, \Delta_3, \Delta_4, \Delta_5)^T$.

Lemma 1. *The Pfaffian vector $\boldsymbol{\Delta}$ belongs to the kernel of the interaction matrix A; that is,*

$$A\boldsymbol{\Delta} = 0.$$

Proof. The statement follows from the standard Pfaffian kernel identity for skew-symmetric matrices of odd order. In the present notation, this identity gives directly $A\boldsymbol{\Delta} = 0$.

Therefore, if

$$\Delta_i > 0, \qquad i = 1, \dots, 5,$$

then the normalized Pfaffian vector determines a positive vector in $\operatorname{Ker} A$. This vector will be used below to construct an interior fixed point of the operator. □

3 Cyclic Face Fixed Points and the Fixed-Point Card

In this section, we describe the fixed points located on the cyclic two-dimensional invariant faces and construct the corresponding fixed-point card. The main purpose is to relate the orientations of the edges of this card to the signs of the Pfaffian invariants introduced above.

Let $J \subset I = \{1, 2, 3, 4, 5\}$. We denote by

$$\Gamma_J = \left\{ x \in S^4 : \ x_i = 0 \text{ for all } i \notin J \right\}$$

the corresponding face of the simplex.

Since the Lotka–Volterra operator has the form

$$x_i' = x_i \left(1 + \sum_{j=1}^{5} a_{ij} x_j \right),$$

each face Γ_J is invariant under V.

For a triple (i, j, k), we write

$$\Gamma_{ijk} = \left\{ x \in S^4 : \ x_l = 0 \text{ for all } l \notin \{i, j, k\} \right\}.$$

The invariant two-dimensional faces corresponding to the cyclic triples identified in the previous section are

$$\Gamma_{135}, \qquad \Gamma_{145}, \qquad \Gamma_{235}, \qquad \Gamma_{245}.$$

Fixed-point properties of Volterra and ℓ-Volterra operators have been studied in [13]. For the cyclic faces considered here, the restriction of V has a unique interior fixed point. These fixed points are

$$C_{135} = \left(\frac{a_{35}}{\delta_{135}}, 0, \frac{a_{15}}{\delta_{135}}, 0, \frac{a_{13}}{\delta_{135}}\right), \qquad \delta_{135} = a_{13} + a_{15} + a_{35}, \tag{5}$$

$$C_{145} = \left(\frac{a_{45}}{\delta_{145}}, 0, 0, \frac{a_{15}}{\delta_{145}}, \frac{a_{14}}{\delta_{145}}\right), \qquad \delta_{145} = a_{14} + a_{15} + a_{45}, \tag{6}$$

$$C_{235} = \left(0, \frac{a_{35}}{\delta_{235}}, \frac{a_{25}}{\delta_{235}}, 0, \frac{a_{23}}{\delta_{235}}\right), \qquad \delta_{235} = a_{23} + a_{25} + a_{35}, \tag{7}$$

and

$$C_{245} = \left(0, \frac{a_{45}}{\delta_{245}}, 0, \frac{a_{25}}{\delta_{245}}, \frac{a_{24}}{\delta_{245}}\right), \qquad \delta_{245} = a_{24} + a_{25} + a_{45}. \tag{8}$$

The fixed points

$$C_{135}, \qquad C_{145}, \qquad C_{235}, \qquad C_{245}$$

form the vertices of the fixed-point card.

In the present configuration, the adjacent pairs are

$$(C_{135}, C_{145}), \qquad (C_{145}, C_{245}), \qquad (C_{245}, C_{235}), \qquad (C_{235}, C_{135}).$$

The orientations of the corresponding edges are determined by the signs of the Pfaffian invariants. According to the orientation criterion established in [7, 8], and with the sign convention adopted in the present paper, we have

$$\Delta_2 > 0 \implies C_{135} \to C_{145}, \tag{9}$$
$$\Delta_3 > 0 \implies C_{145} \to C_{245}, \tag{10}$$
$$\Delta_1 > 0 \implies C_{245} \to C_{235}, \tag{11}$$
$$\Delta_4 > 0 \implies C_{235} \to C_{135}. \tag{12}$$

Therefore, if

$$\Delta_i > 0, \qquad i = 1, 2, 3, 4,$$

then the four vertices form the directed cycle

$$C_{135} \to C_{145} \to C_{245} \to C_{235} \to C_{135}.$$

According to the criterion established in [14], such a cyclic fixed-point card implies the existence of an interior fixed point. In the next section, this point is constructed explicitly using the Pfaffian vector.

4 Cyclic Fixed-Point Card, Interior Fixed Point and Local Spectrum

In this section, we study the cyclic fixed-point card considered above, construct the corresponding interior fixed point, and analyze the local spectrum of the operator at this point.

Assume that all Pfaffian invariants are positive:

$$\Delta_i > 0, \qquad i = 1, \dots, 5. \tag{13}$$

In particular,

$$\Delta_1, \Delta_2, \Delta_3, \Delta_4 > 0.$$

Therefore, by the orientation relations (9)–(12), the four fixed points located on the cyclic two-dimensional invariant faces form the directed cyclic fixed-point card

$$C_{135} \to C_{145} \to C_{245} \to C_{235} \to C_{135}.$$

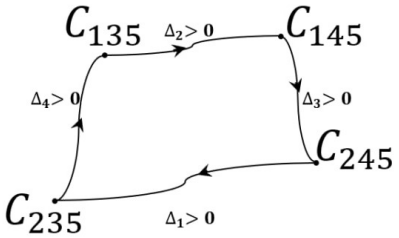


Figure 2 Directed cyclic fixed-point card in the case $\Delta_i > 0$, $i = 1, 2, 3, 4$.

The cyclic structure of the card is determined by the signs of the Pfaffian invariants $\Delta_1, \Delta_2, \Delta_3, \Delta_4$. Under condition (13), the full Pfaffian vector

$$\mathbf{\Delta} = (\Delta_1, \Delta_2, \Delta_3, \Delta_4, \Delta_5)^T$$

has strictly positive components. Criteria relating fixed-point cards to the existence of interior fixed points were established in [14]. We now construct the interior fixed point explicitly using the Pfaffian vector.

Put

$$\Delta = \Delta_1 + \Delta_2 + \Delta_3 + \Delta_4 + \Delta_5. \tag{14}$$

By (13), $\Delta > 0$.

Theorem 2. *Assume that*

$$\Delta_i > 0, \qquad i = 1, \dots, 5.$$

Then the Lotka–Volterra operator (3) *has the interior fixed point*

$$x^* = \left(\frac{\Delta_1}{\Delta}, \frac{\Delta_2}{\Delta}, \frac{\Delta_3}{\Delta}, \frac{\Delta_4}{\Delta}, \frac{\Delta_5}{\Delta} \right).$$

Proof. Since

$$\Delta_i > 0, \qquad i = 1, \dots, 5,$$

all coordinates of x^* are positive. Moreover,

$$\sum_{i=1}^{5} x_i^* = \frac{\Delta_1 + \Delta_2 + \Delta_3 + \Delta_4 + \Delta_5}{\Delta} = 1.$$

Hence,

$$x^* \in \operatorname{Int} S^4.$$

By Lemma 1, the Pfaffian vector satisfies

$$A\boldsymbol{\Delta} = 0.$$

Since

$$x^* = \frac{\boldsymbol{\Delta}}{\Delta},$$

it follows that

$$Ax^* = 0.$$

Thus, for every

$$i = 1, \dots, 5,$$

we have

$$\sum_{j=1}^{5} a_{ij} x_j^* = 0.$$

Substituting this equality into the Lotka–Volterra formula gives

$$(Vx^*)_i = x_i^* \left(1 + \sum_{j=1}^{5} a_{ij} x_j^*\right) = x_i^*.$$

Therefore,

$$Vx^* = x^*,$$

and hence x^* is an interior fixed point of V. □

We next analyze the local spectrum of the operator at x^*.
For the Lotka–Volterra operator

$$(Vx)_i = x_i \left(1 + \sum_{j=1}^{5} \alpha_{ij} x_j\right),$$

the entries of the Jacobian matrix are

$$J_{ij}(x) = \frac{\partial (Vx)_i}{\partial x_j} = \delta_{ij} \left(1 + \sum_{k=1}^{5} \alpha_{ik} x_k\right) + x_i \alpha_{ij}.$$

At the fixed point x^*, the equality

$$Ax^* = 0$$

implies

$$1 + \sum_{k=1}^{5} \alpha_{ik} x_k^* = 1.$$

Therefore,

$$J(x^*) = I + D_* A, \tag{15}$$

where

$$D_* = \operatorname{diag}(x_1^*, x_2^*, x_3^*, x_4^*, x_5^*).$$

Equivalently,

$$D_* = \operatorname{diag}\left(\frac{\Delta_1}{\Delta}, \frac{\Delta_2}{\Delta}, \frac{\Delta_3}{\Delta}, \frac{\Delta_4}{\Delta}, \frac{\Delta_5}{\Delta}\right).$$

We now determine the characteristic polynomial of $J(x^*)$.

Theorem 3. *Assume that*

$$\Delta_i > 0, \qquad i = 1, \dots, 5.$$

Then

$$D(\lambda) = \det(J(x^*) - \lambda I)$$

has the form

$$D(\lambda) = (1-\lambda)\left[(1-\lambda)^4 + S_2(1-\lambda)^2 + S_4\right], \tag{16}$$

where

$$S_2 = \frac{1}{\Delta^2} \sum_{1 \leqslant i < j \leqslant 5} a_{ij}^2 \Delta_i \Delta_j, \tag{17}$$

and

$$S_4 = \frac{\Delta_1 \Delta_2 \Delta_3 \Delta_4 \Delta_5}{\Delta^3}. \tag{18}$$

Proof. From (15),

$$J(x^*) - \lambda I = (1-\lambda) I + D_* A.$$

Let

$$\mu = 1 - \lambda.$$

Then

$$D(\lambda) = \det(\mu I + D_* A).$$

Since D_* is a positive diagonal matrix, $D_* A$ is similar to

$$K = D_*^{1/2} A D_*^{1/2}.$$

Indeed,

$$D_*^{-1/2}(D_* A) D_*^{1/2} = D_*^{1/2} A D_*^{1/2} = K.$$

Since

$$A^T = -A,$$

we obtain

$$K^T = \left(D_*^{1/2} A D_*^{1/2}\right)^T = D_*^{1/2} A^T D_*^{1/2} = -K.$$

Thus K is a real skew-symmetric 5×5 matrix. Consequently, its eigenvalues have the form

$$0, \qquad \pm i\omega_1, \qquad \pm i\omega_2,$$

and therefore

$$\det(\mu I + K) = \mu\left(\mu^4 + S_2 \mu^2 + S_4\right).$$

Since $D_* A$ and K are similar,

$$\det(\mu I + D_* A) = \det(\mu I + K).$$

Hence,

$$D(\lambda) = \mu\left(\mu^4 + S_2 \mu^2 + S_4\right).$$

Using

$$\mu = 1 - \lambda,$$

we obtain

$$D(\lambda) = (1-\lambda)\left[(1-\lambda)^4 + S_2(1-\lambda)^2 + S_4\right].$$

The coefficient S_2 is the sum of the second-order principal contributions of the weighted skew-symmetric matrix K:

$$S_2 = \sum_{1 \leqslant i < j \leqslant 5} a_{ij}^2 x_i^* x_j^*.$$

Since

$$x_i^* = \frac{\Delta_i}{\Delta},$$

we obtain

$$S_2 = \frac{1}{\Delta^2} \sum_{1 \leqslant i < j \leqslant 5} a_{ij}^2 \Delta_i \Delta_j.$$

The fourth-order coefficient is the sum of the fourth-order principal contributions of K. Since the fourth-order principal Pfaffians of A are represented by the quantities Δ_i, we have

$$S_4 = \sum_{i=1}^{5} \left(\prod_{j \neq i} x_j^* \right) \Delta_i^2.$$

Substituting

$$x_j^* = \frac{\Delta_j}{\Delta},$$

we obtain

$$S_4 = \sum_{i=1}^{5} \left(\prod_{j \neq i} \frac{\Delta_j}{\Delta} \right) \Delta_i^2.$$

Therefore,

$$S_4 = \frac{\Delta_1 \Delta_2 \Delta_3 \Delta_4 \Delta_5}{\Delta^4} \sum_{i=1}^{5} \Delta_i.$$

By (14),

$$\sum_{i=1}^{5} \Delta_i = \Delta.$$

Hence,

$$S_4 = \frac{\Delta_1 \Delta_2 \Delta_3 \Delta_4 \Delta_5}{\Delta^3}.$$

Thus, (16) follows. □

Remark 1. The characteristic polynomial is expressed entirely through the interaction coefficients a_{ij} and the Pfaffian invariants Δ_i. Thus, the same algebraic quantities determine both the cyclic structure of the fixed-point card and the local spectrum at the interior fixed point.

We now describe the eigenvalues explicitly.

From (16), one eigenvalue of the full Jacobian matrix is

$$\lambda_0 = 1.$$

The remaining four eigenvalues are determined by

$$(1 - \lambda)^4 + S_2 (1 - \lambda)^2 + S_4 = 0.$$

Putting again

$$\mu = 1 - \lambda,$$

we obtain the biquadratic equation

$$\mu^4 + S_2\mu^2 + S_4 = 0. \tag{19}$$

Since D_*A is similar to the real skew-symmetric matrix K, its two nonzero pairs of eigenvalues are purely imaginary. Therefore, the four nontrivial eigenvalues of

$$J(x^*) = I + D_*A$$

have the form

$$1 \pm i\omega_1, \qquad 1 \pm i\omega_2.$$

More precisely,

$$\omega_{1,2}^2 = \frac{S_2 \pm \sqrt{S_2^2 - 4S_4}}{2}.$$

Moreover,

$$S_2^2 - 4S_4 \geqslant 0,$$

because

$$S_2 = \omega_1^2 + \omega_2^2, \qquad S_4 = \omega_1^2\omega_2^2,$$

and hence

$$S_2^2 - 4S_4 = (\omega_1^2 - \omega_2^2)^2 \geqslant 0.$$

Since $\Delta_i > 0$ for all $i = 1, \ldots, 5$, formula (18) gives

$$S_4 > 0.$$

Consequently,

$$\omega_1^2\omega_2^2 = S_4 > 0,$$

and therefore

$$\omega_1 > 0, \qquad \omega_2 > 0.$$

Theorem 4. *Under assumption* (13)*, the spectrum of the full Jacobian matrix* $J(x^*)$ *is*

$$\operatorname{spec}(J(x^*)) = \{1,\ 1 \pm i\omega_1,\ 1 \pm i\omega_2\},$$

where

$$\omega_{1,2}^2 = \frac{S_2 \pm \sqrt{S_2^2 - 4S_4}}{2}. \tag{20}$$

Moreover,

$$\omega_1 > 0, \qquad \omega_2 > 0.$$

Proof. The factor

$$1 - \lambda$$

in (16) gives the eigenvalue

$$\lambda_0 = 1.$$

The remaining four eigenvalues satisfy (19). Solving this equation with respect to μ^2, we obtain

$$\mu^2 = \frac{-S_2 \pm \sqrt{S_2^2 - 4S_4}}{2}.$$

Since the corresponding eigenvalues of D_*A are purely imaginary, we may write

$$\mu = \pm i\omega_1, \qquad \mu = \pm i\omega_2.$$

Since

$$\lambda = 1 - \mu,$$

we obtain

$$\operatorname{spec}(J(x^*)) = \{1,\ 1 \pm i\omega_1,\ 1 \pm i\omega_2\}.$$

Formula (20) follows directly from the quadratic equation for μ^2.

Finally, since

$$S_4 = \omega_1^2\omega_2^2 = \frac{\Delta_1\Delta_2\Delta_3\Delta_4\Delta_5}{\Delta^3} > 0,$$

both frequencies are strictly positive:

$$\omega_1 > 0, \qquad \omega_2 > 0.$$

□

We now take into account that the dynamics of V is restricted to the four-dimensional simplex S^4. The tangent space to the simplex at x^* is

$$T_{x^*}S^4 = \left\{ h = (h_1, \ldots, h_5) \in \mathbb{R}^5 : \sum_{i=1}^{5} h_i = 0 \right\}.$$

We first show that the tangent space $T_{x^*}S^4$ is invariant under the Jacobian $J(x^*)$.

Since A is skew-symmetric, for every $x \in \mathbb{R}^5$ we have

$$x^T A x = 0.$$

Therefore,

$$\sum_{i=1}^{5}(Vx)_i = \sum_{i=1}^{5} x_i \left(1 + \sum_{j=1}^{5} a_{ij}x_j\right) = \sum_{i=1}^{5} x_i + x^T A x = \sum_{i=1}^{5} x_i.$$

Differentiating this identity with respect to x, we obtain

$$\mathbf{1}^T J(x) = \mathbf{1}^T,$$

where

$$\mathbf{1} = (1, 1, 1, 1, 1)^T.$$

Hence, for every

$$h \in T_{x^*}S^4,$$

we have

$$\mathbf{1}^T h = 0,$$

and therefore

$$\mathbf{1}^T J(x^*)h = \mathbf{1}^T h = 0.$$

Thus,

$$J(x^*)h \in T_{x^*}S^4$$

for every $h \in T_{x^*}S^4$. Consequently,

$$J(x^*)T_{x^*}S^4 \subseteq T_{x^*}S^4.$$

Hence, the tangent space $T_{x^*}S^4$ is invariant under the Jacobian $J(x^*)$.

We next identify the eigenvector corresponding to the eigenvalue $\lambda_0 = 1$. By Lemma 1,

$$A\boldsymbol{\Delta} = 0.$$

Consequently,

$$D_* A\boldsymbol{\Delta} = 0,$$

and therefore

$$J(x^*)\boldsymbol{\Delta} = (I + D_* A)\boldsymbol{\Delta} = \boldsymbol{\Delta}.$$

Thus, $\boldsymbol{\Delta}$ is an eigenvector of $J(x^*)$ corresponding to the eigenvalue $\lambda_0 = 1$.

Moreover,

$$\mathbf{1}^T\boldsymbol{\Delta} = \Delta_1 + \Delta_2 + \Delta_3 + \Delta_4 + \Delta_5 = \Delta > 0.$$

Hence,

$$\boldsymbol{\Delta} \notin T_{x^*}S^4.$$

Thus, the eigenvalue $\lambda_0 = 1$ corresponds to a direction transverse to the tangent space of the simplex.

Furthermore, since $S_4 > 0$, the factor

$$(1-\lambda)^4 + S_2(1-\lambda)^2 + S_4$$

does not vanish at $\lambda = 1$. Therefore, the eigenvalue $\lambda_0 = 1$ is simple.

Since $T_{x^*}S^4$ is a four-dimensional invariant subspace and the eigenvector corresponding to the simple eigenvalue $\lambda_0 = 1$ does not belong to this tangent space, the spectrum of the restriction of the Jacobian to $T_{x^*}S^4$ consists precisely of the remaining four eigenvalues:

$$\operatorname{spec}\left(J(x^*)\big|_{T_{x^*}S^4}\right) = \{1 \pm i\omega_1,\ 1 \pm i\omega_2\}.$$

Corollary 1. *Under assumption* (13)*, the interior fixed point x^* is locally repelling with respect to the dynamics on the simplex S^4.*

Indeed, the four eigenvalues of the tangent restriction satisfy

$$|1 \pm i\omega_k| = \sqrt{1+\omega_k^2} > 1, \qquad k = 1, 2.$$

Hence all tangent spectral directions are expanding.

Proof. Since

$$\omega_k > 0, \qquad k = 1, 2,$$

we have

$$|1 \pm i\omega_k| = \sqrt{1+\omega_k^2} > 1.$$

Thus every eigenvalue of the restricted Jacobian

$$J(x^*)\big|_{T_{x^*}S^4}$$

lies outside the unit circle. Therefore the interior fixed point is locally repelling on S^4.

Since the eigenvalues occur in complex conjugate pairs, the local repelling dynamics also contains rotational, or oscillatory, components. □

Remark 2. The interior fixed point x^* represents a balance point generated by the positive Pfaffian vector, but it is not an attracting equilibrium. The fixed-point card describes the cyclic structure of the boundary fixed points, while the spectrum of the Jacobian restricted to $T_{x^*}S^4$ shows that the local dynamics near the interior fixed point has an oscillatory repelling character.

In applications, this spectral structure corresponds to cyclic redistribution around the balance state rather than monotone convergence to a single static distribution.

5 Mathematical Formulation of Integrated Geological Evidence

The theoretical construction developed above can be incorporated into a mathematical framework for the integration of heterogeneous geological evidence used in gold prospectivity analysis. Mineral prospectivity assessment generally requires the simultaneous interpretation of several types of geological, geochemical, geophysical, and structural information [15, 16]. In the present framework, these heterogeneous data are represented by five aggregated evidence groups:

$$E_1 = \text{geochemical evidence}, \qquad E_2 = \text{geophysical evidence},$$

$$E_3 = \text{structural evidence}, \qquad E_4 = \text{lithological–formation evidence},$$

and

$$E_5 = \text{mineralogical–alteration evidence}.$$

The integration of these evidence groups requires attention to spatial alignment, measurement scale, and differences in data resolution, as emphasized in recent work on multimodal mineral system characterization [17].

Remote-sensing information may additionally contribute to the construction of the structural, lithological, and alteration evidence groups [18]. Thus, the five-dimensional representation should be understood as an integration of information sources rather than as a restriction to five individual geological variables.

Let

$$z = (z_1, z_2, z_3, z_4, z_5)$$

denote the aggregated nonnegative evidence values at a given spatial location. After preprocessing and normalization, we define

$$x_i = \frac{z_i}{\sum_{j=1}^{5} z_j}, \qquad i = 1, \ldots, 5, \tag{21}$$

provided that

$$\sum_{j=1}^{5} z_j > 0.$$

Hence,

$$x = (x_1, \ldots, x_5) \in S^4.$$

The simplex representation has a natural interpretation: each coordinate x_i describes the relative contribution of the corresponding geological evidence group at the considered spatial location. Therefore, different locations are represented by different points of the same four-dimensional simplex.

The interaction matrix

$$A = (a_{ij})_{i,j=1}^{5}, \qquad A^T = -A,$$

describes the pairwise interaction structure of the five evidence groups. The coefficient a_{ij} represents the signed relative interaction between the i-th and j-th groups, while its magnitude characterizes the strength of this interaction.

In a practical implementation, the magnitudes of the interaction coefficients may be estimated from spatial or statistical relations between the corresponding evidence groups, whereas their signs are required to satisfy the interaction pattern prescribed by the theoretical Lotka–Volterra configuration considered in this paper. Thus, the resulting matrix combines empirical information with the structural constraints of the mathematical model.

Knowledge-driven, data-driven, and hybrid evidence-integration approaches have been applied to gold prospectivity mapping, including weights-of-evidence and fuzzy-logic models [19].

For a geological evidence profile $x \in S^4$, define the interaction response vector

$$q(x) = Ax. \tag{22}$$

Its components

$$q_i(x) = \sum_{j=1}^{5} a_{ij} x_j$$

measure the net interaction effect acting on the i-th evidence group.

The corresponding one-step Lotka–Volterra redistribution is

$$V(x) = x + \operatorname{diag}(x)Ax, \tag{23}$$

or componentwise,

$$(Vx)_i = x_i \left(1 + q_i(x)\right).$$

Therefore, the vector

$$R(x) = V(x) - x = \operatorname{diag}(x)Ax \tag{24}$$

provides a quantitative measure of the interaction-induced redistribution of the geological evidence profile.

Unlike a purely additive evidence model, relation (24) takes into account pairwise interactions between the different sources of geological information. Consequently, two locations having similar individual evidence values may produce different interaction responses if the relative configuration of their evidence components is different.

The algebraic structure of these interactions is further characterized by the Pfaffian invariants

$$\Delta_1, \ldots, \Delta_5.$$

When

$$\Delta_i > 0, \qquad i = 1, \ldots, 5,$$

the model possesses the interior fixed point

$$x^* = \frac{1}{\Delta}(\Delta_1, \Delta_2, \Delta_3, \Delta_4, \Delta_5), \qquad \Delta = \sum_{i=1}^{5} \Delta_i.$$

In the geological interpretation, x^* is a model-defined reference configuration at which the net interaction response vanishes:

$$Ax^* = 0, \qquad R(x^*) = 0.$$

Thus, x^* characterizes a balanced interaction state of the five normalized evidence groups.

It is important to distinguish this interpretation from dynamical stability. As shown in the previous section, x^* is locally repelling for the discrete Lotka–Volterra dynamics on S^4. Therefore, closeness to x^* is not identified directly with high gold prospectivity. Instead, x^* serves as a mathematically defined reference configuration for measuring and comparing different geological evidence structures.

6 Model-Based Descriptors and a Proposed Computational Scheme

To connect the Lotka–Volterra structure with spatial prospectivity analysis, we introduce a collection of model-based descriptors associated with each geological evidence profile $x \in S^4$.

The first descriptor is the distance from the interior reference state,

$$d_*(x) = \|x - x^*\|_2. \tag{25}$$

This quantity measures the deviation of the observed evidence composition from the balanced interaction configuration.

The second descriptor is the magnitude of the interaction response,

$$I(x) = \|Ax\|_2. \tag{26}$$

Since

$$Ax^* = 0,$$

we have

$$I(x^*) = 0.$$

Large values of $I(x)$ indicate evidence configurations in which the pairwise interaction structure generates a stronger net response.

A third descriptor is obtained from the actual Lotka–Volterra redistribution,

$$L(x) = \|V(x) - x\|_2 = \|\operatorname{diag}(x)Ax\|_2. \tag{27}$$

Unlike $I(x)$, the quantity $L(x)$ also accounts for the relative weight of each evidence component through the factors x_i.

The boundary fixed points

$$C_{135}, \qquad C_{145}, \qquad C_{245}, \qquad C_{235}$$

provide additional reference configurations corresponding to the cyclic two-dimensional invariant faces. For each of them, define

$$d_{ijk}(x) = \|x - C_{ijk}\|_2.$$

The vector

$$D_C(x) = (d_{135}(x), d_{145}(x), d_{245}(x), d_{235}(x)) \tag{28}$$

therefore describes the position of a geological evidence profile relative to the cyclic fixed-point card.

The resulting Lotka–Volterra prospectivity descriptor is defined as

$$\Phi(x) = (x_1, \dots, x_5,\, d_*(x),\, I(x),\, L(x),\, D_C(x))\,. \tag{29}$$

Thus, $\Phi(x)$ contains three complementary types of information: the normalized geological composition, the interaction response generated by the skew-symmetric matrix, and the position of the evidence profile relative to the interior and boundary fixed-point configurations.

For quantitative prospectivity assessment, we propose a calibrated prospectivity functional of the general form

$$P(x) = G\big(\Phi(x); \theta\big), \qquad 0 \leqslant P(x) \leqslant 1, \tag{30}$$

where G is a monotone calibration function and θ denotes parameters determined from exploration observations.

The introduction of G is essential. The mathematical theory determines the interaction structure and the descriptors in (29), but it does not by itself determine which numerical combination of these quantities corresponds to economically significant gold mineralization. This relation must be established using geological observations.

A simple parametric realization is

$$P(x) = \frac{1}{1 + \exp\left[-\left(\beta_0 + \sum_{k=1}^{m} \beta_k \Phi_k(x)\right)\right]}, \tag{31}$$

where the coefficients

$$\beta_0, \beta_1, \dots, \beta_m$$

are calibrated using known mineralized and background locations.

Equation (31) is not part of the Lotka–Volterra dynamics itself. Rather, it provides a statistical calibration layer connecting the deterministic dynamical descriptors with observed mineralization data. Other calibrated mappings may be used without changing the underlying Pfaffian–Lotka–Volterra construction.

The complete computational procedure can therefore be organized as follows.

1. Collect geochemical, geophysical, structural, lithological–formation, and mineralogical–alteration information for each spatial observation.
2. Preprocess the heterogeneous variables and aggregate them into five nonnegative evidence groups
$$z_1, \dots, z_5.$$
3. Transform each observation into a point of the simplex using
$$x_i = \frac{z_i}{\sum_{j=1}^{5} z_j}.$$
4. Construct or estimate the skew-symmetric interaction matrix
$$A = (a_{ij}), \qquad A^T = -A,$$
subject to the sign structure of the Lotka–Volterra configuration.

5. Compute the Pfaffian invariants
$$\Delta_1, \ldots, \Delta_5$$
and determine the orientation of the corresponding fixed-point card.
6. When
$$\Delta_i > 0, \qquad i = 1, \ldots, 5,$$
construct the interior fixed point
$$x^* = \frac{1}{\Delta}(\Delta_1, \ldots, \Delta_5).$$
7. Compute the model-based descriptors
$$d_*(x), \qquad I(x), \qquad L(x), \qquad D_C(x)$$
for every spatial observation.
8. Calibrate the prospectivity functional
$$P(x) = G(\Phi(x); \theta)$$
against known mineral occurrences, deposits, or other reliable exploration targets.
9. Apply the calibrated model to the study region and classify the resulting values of $P(x)$ into prospectivity classes.
10. Validate the resulting prospectivity pattern using observations not employed in the calibration stage and evaluate the sensitivity of the results to data preprocessing, parameter estimation, and uncertainty.

Uncertainty analysis is particularly important in mineral prospectivity mapping because preprocessing choices and the construction of evidence layers may influence the final spatial prediction [20, 21]. The representativeness of known mineralized and non-mineralized observations must also be considered during calibration and validation [22].

The selection of background or non-deposit locations also requires careful consideration, because it can influence the performance of gold prospectivity models [23].

The proposed formulation therefore separates three distinct levels of the model:

$$\boxed{\begin{array}{c}\text{geological evidence} \longrightarrow \text{Lotka–Volterra/Pfaffian structure} \\ \longrightarrow \text{calibrated prospectivity assessment}\end{array}}.$$

The first level provides the spatial evidence variables, the second describes their nonlinear interaction geometry, and the third establishes the empirical relation between the mathematical descriptors and actual gold mineralization.

This separation avoids identifying dynamical equilibrium with geological favorability while retaining the Pfaffian and spectral structure as the mathematical core of the prospectivity model. It also makes the framework suitable for subsequent implementation using real spatial exploration data and for comparison with alternative mineral prospectivity methods [24].

7 A Synthetic Numerical Experiment

This section provides a reproducible numerical illustration of the theoretical results and the proposed evidence descriptors. All coefficients and profiles are synthetic; no exploration observations, measured concentrations, deposit labels, or spatial prediction

outputs are used. The experiment verifies the algebraic calculations and illustrates the computation of descriptors. It does not assess gold prediction accuracy.

7.1 Interaction matrix and fixed-point configurations

We choose the interaction matrix

$$A = \begin{pmatrix} 0 & -0.3 & -0.1 & -0.6 & 0.9 \\ 0.3 & 0 & -0.9 & -0.3 & 0.3 \\ 0.1 & 0.9 & 0 & -0.1 & -0.2 \\ 0.6 & 0.3 & 0.1 & 0 & -0.5 \\ -0.9 & -0.3 & 0.2 & 0.5 & 0 \end{pmatrix}.$$

Its entries satisfy the sign pattern in (4), skew symmetry, and $|\alpha_{ij}| \leqslant 1$. Substitution into the Pfaffian formulas gives

$$\mathbf{\Delta} = (0.36, 0.16, 0.06, 0.72, 0.54)^T, \qquad \Delta = 1.84.$$

All five components are positive. Consequently, the prescribed card has cyclic orientation and the interior fixed point is

$$x^* = \frac{1}{184}(36, 16, 6, 72, 54)^T = (0.195652, 0.086957, 0.032609, 0.391304, 0.293478)^T.$$

Direct computation gives $Ax^* = 0$ and $V(x^*) = x^*$, up to floating-point roundoff. The four face fixed points are

$$C_{135} = \frac{1}{12}(2, 0, 9, 0, 1), \qquad C_{145} = \frac{1}{20}(5, 0, 0, 9, 6),$$
$$C_{245} = \frac{1}{11}(0, 5, 0, 3, 3), \qquad C_{235} = \frac{1}{14}(0, 2, 3, 0, 9).$$

Each satisfies $V(C_{ijk}) = C_{ijk}$. These configurations are reference compositions defined by the model; their coordinates are not measured geological concentrations.

7.2 Spectrum and local departure

For $J(x^*) = I + \operatorname{diag}(x^*)A$, the characteristic coefficients are

$$S_2 = 0.112542533, \qquad S_4 = 0.000215698.$$

The ambient eigenvalues, rounded to six decimal places, are

$$\lambda_0 = 1, \qquad \lambda_{1,2} = 1 \pm 0.044163i, \qquad \lambda_{3,4} = 1 \pm 0.332554i.$$

The two corresponding moduli are 1.000975 and 1.053846. The four non-unit eigenvalues lie outside the unit circle. The eigenvalue 1 corresponds to the transverse eigenvector x^* and is excluded when restricting the Jacobian to TS^4. Thus, the computed spectrum agrees with local repulsion on the simplex.

To illustrate this behavior, let

$$x^{(0)} = x^* + 10^{-3}u, \qquad u = \frac{1}{\sqrt{2}}(1, -1, 0, 0, 0)^T,$$

and iterate $x^{(n+1)} = V(x^{(n)})$ for $0 \leqslant n < 400$. Since $\sum_i u_i = 0$ and all initial coordinates are positive, the initial condition belongs to $\operatorname{Int} S^4$. No additional normalization or

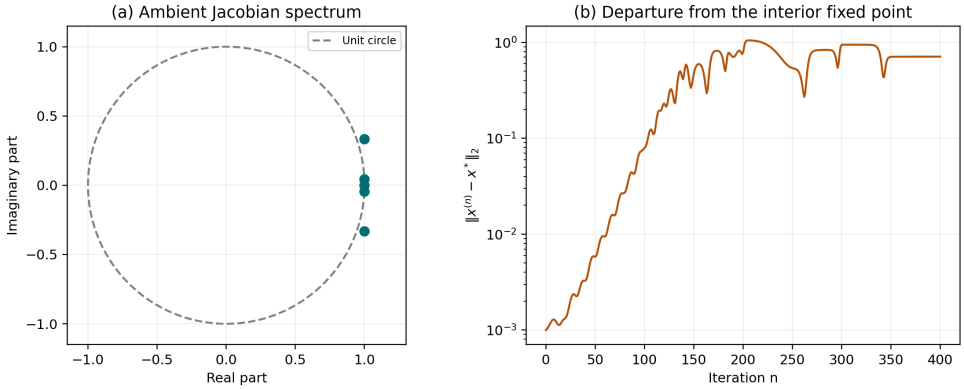


Figure 3 Synthetic experiment: (a) ambient Jacobian eigenvalues and the unit circle; (b) distance from the interior fixed point along a perturbed trajectory. The transverse eigenvalue 1 is displayed in (a) but does not belong to the tangent spectrum.

projection is applied during iteration. The initial distance is 10^{-3}, and the distance at iteration 400 is 0.709596. Figure 3 displays the spectrum and the computed departure. This finite trajectory illustrates local instability; it does not establish a global convergence statement or imply monotone distance growth for every initial condition.

7.3 Descriptors for synthetic evidence profiles

We consider seven normalized profiles $P_0, \ldots, P_6$, with $P_0 = x^*$. The five coordinates represent the five evidence groups in the proposed framework, rather than five measured element concentrations. Table 1 reports their coordinates and descriptors. Values are rounded independently to four decimal places; all calculations use unrounded values. At P_0, the three descriptors vanish. For the remaining profiles, the values distinguish

Table 1 Synthetic compositions and computed descriptors.

Profile	x_1	x_2	x_3	x_4	x_5	d_*	I	L
P0	0.1957	0.0870	0.0326	0.3913	0.2935	0.0000	0.0000	0.0000
P1	0.2000	0.2000	0.2000	0.2000	0.2000	0.2935	0.2332	0.0466
P2	0.4500	0.1500	0.1000	0.1000	0.2000	0.4084	0.4709	0.0862
P3	0.1000	0.4000	0.1500	0.1000	0.2500	0.4557	0.3499	0.0621
P4	0.1000	0.1000	0.4000	0.1500	0.2500	0.4521	0.3110	0.0349
P5	0.1000	0.1000	0.1500	0.4000	0.2500	0.1583	0.1967	0.0329
P6	0.1000	0.1000	0.1000	0.1000	0.6000	0.4389	0.4951	0.0577

compositional displacement, net interaction response, and actual one-step redistribution. Figure 4 compares these values. The four distances to the face fixed points are also computed and supplied in the accompanying numerical results file.

The experiment confirms consistency between the Pfaffian construction, direct fixed-point calculations, and the local spectrum for the selected matrix. It also demonstrates a fully specified computation of the proposed evidence descriptors. No prospectivity functional G, probability estimate, classification threshold, or prediction-quality metric is fitted because observed mineralization labels are unavailable in this synthetic experiment. Establishing geological usefulness requires a separate study with documented exploration data and independent validation.

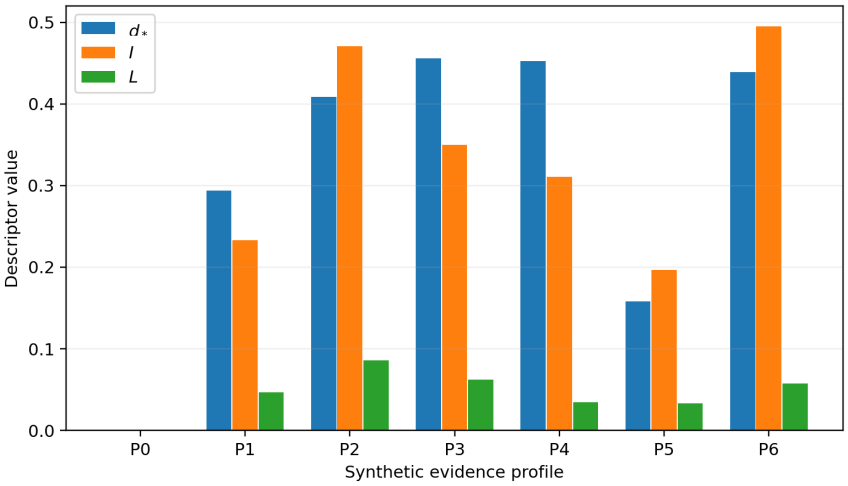


Figure 4 Distances and interaction descriptors for seven synthetic evidence profiles. Larger values indicate larger model-defined deviations or responses; they do not imply greater gold prospectivity.

8 Conclusion

This study examined the connection between the Pfaffian structure of a discrete Lotka–Volterra operator, its cyclic fixed-point card, and the local dynamics at an interior fixed point on the four-dimensional simplex. The four cyclic two-dimensional invariant faces provide the fixed points forming the vertices of the card. Under the adopted sign convention, the established orientation criterion relates the signs of the relevant fourth-order principal Pfaffian invariants to the directed cycle of these vertices.

Positivity of the full Pfaffian vector gives an explicit interior fixed point through normalized Pfaffian ratios. The characteristic polynomial of the Jacobian at this point was expressed in terms of the interaction coefficients and the same Pfaffian invariants. The tangent space of the simplex is invariant under the Jacobian. Its restricted spectrum consists of two complex conjugate pairs with moduli greater than one, whereas the simple eigenvalue equal to one belongs to a transverse direction in the ambient space. Thus, the interior fixed point is locally repelling on the simplex, with oscillatory components in its local dynamics.

A possible interpretation of this mathematical construction was proposed for integrating five groups of geological evidence. In this interpretation, the interior fixed point serves as a model-defined reference composition, while distances to the interior and face fixed points, together with interaction-response measures, describe the relative configuration of the evidence. These descriptors do not by themselves establish geological favorability or constitute a validated gold prospectivity model.

Further application requires explicit construction of the evidence variables, estimation of the interaction coefficients under the prescribed structural constraints, and verification of the Pfaffian positivity conditions. Any relationship between the proposed descriptors and gold mineralization must then be calibrated and tested using independent exploration observations. The present results therefore provide a mathematical foundation and a proposed computational scheme for future geological evidence integration studies.

Declarations

Funding. This research received no external funding.

Conflicts of interest. The authors declare no conflict of interest.

Author contributions. D. B. Eshmamatova: conceptualization, methodology, and supervision; K. A. Solijanova: mathematical analysis, computational investigation, and writing of the original draft. Both authors reviewed and approved the final manuscript.

Data availability. The mathematical results and formulas are presented in the article. Access to the geological data is subject to the conditions established by the data providers.

References

[1] Lyubich Yu. I. 1992. *Mathematical Structures in Population Genetics*. Springer-Verlag, Berlin, Biomathematics, Vol. 22.

[2] Ganikhodzhaev R. N. 1993. Quadratic stochastic operators, Lyapunov functions, and tournaments. *Russian Academy of Sciences. Sbornik Mathematics*. 76(2): 489–506. doi: https://doi.org/10.1070/SM1993v076n02ABEH003423.

[3] Eshmamatova D. B. 2022. Compositions of Lotka–Volterra mappings operating in a two-dimensional simplex, relation to viral diseases and their numerical analysis. *Problems of Computational and Applied Mathematics*. 3(41): 79–92.

[4] Moon J. W. 1968. *Topics on Tournaments*. Holt, Rinehart and Winston, New York.

[5] Tadzhieva M. A., Eshmamatova D. B., Ganikhodzhaev R. N. 2024. Volterra-type quadratic stochastic operators with a homogeneous tournament. *Journal of Mathematical Sciences*. 278(3): 546–556. doi: https://doi.org/10.1007/s10958-024-06937-0.

[6] Ganikhodzhaev R. N., Kurganov K. A., Tadzhieva M. A., Khaidarov F. Kh. 2024. Dynamics of quadratic Volterra-type stochastic operators corresponding to strange tournaments. *Vladikavkaz Mathematical Journal*. 26(1): 85–99. doi: https://doi.org/10.46698/n9080-6847-9986-u.

[7] Eshmamatova D. B., Tadzhieva M. A. 2024. Cards of fixed points of some Lotka–Volterra operators. *e-Journal of Analysis and Applied Mathematics*. 2024: 71–80. doi: https://doi.org/10.62780/ejaam/2024-006.

[8] Solijanova K. 2026. Spectral Properties and Fixed Point Structure of a Lotka–Volterra Operator on the Four-Dimensional Simplex. *Journal of Mathematical Sciences*. Online first. doi: https://doi.org/10.1007/s10958-026-08434-y.

[9] Solijanova K. 2026. Degenerate Fixed-Point Configurations of a Discrete Lotka–Volterra Operator. *Journal of Mathematical Sciences*. Online first. doi: https://doi.org/10.1007/s10958-026-08610-0.

[10] Geiger P. M., Knebel J., Frey E. 2018. Topologically robust zero-sum games and Pfaffian orientation: How network topology determines the long-time dynamics of the antisymmetric Lotka–Volterra equation. *Physical Review E*. 98. doi: https://doi.org/10.1103/PhysRevE.98.062316.

[11] Eshmamatova D. B. 2022. Discrete models of viral diseases with reinfection transmitted by the airborne droplet route. *Problems of Computational and Applied Mathematics*. 4(42): 36–54.

[12] Horn R. A., Johnson C. R. 2013. *Matrix Analysis*. 2nd ed., Cambridge University Press, Cambridge.

[13] Yusupov F. A. 2024. Modeling the dynamics of computer virus spread using compositions of Lotka–Volterra mappings. *Problems of Computational and Applied Mathematics*. 3(57): 122–139.

[14] Eshmamatova D. B., Tadzhieva M. A., Ganikhodzhaev R. N. 2022. Criteria for internal fixed points existence of discrete dynamic Lotka–Volterra systems with homogeneous tournaments. *Izvestiya VUZ. Applied Nonlinear Dynamics*. 30(6): 702–716. doi: https://doi.org/10.18500/0869-6632-003012.

[15] Carranza E. J. M. 2008. *Geochemical Anomaly and Mineral Prospectivity Mapping in GIS*. Elsevier, Amsterdam, Handbook of Exploration and Environmental Geochemistry, Vol. 11.

[16] Zuo R., Carranza E. J. M. 2023. Machine learning-based mapping for mineral exploration. *Mathematical Geosciences*. 55: 891–895. doi: https://doi.org/10.1007/s11004-023-10097-3.

[17] Austin J. R., Gazley M., Birchall R. [et al.] 2024. Integration by design: driving mineral system knowledge using multi-modal, collocated, scale-consistent characterisation. *Earth System Science Data*. 16: 5027–5067. doi: https://doi.org/10.5194/essd-16-5027-2024.

[18] Shirmard H., Farahbakhsh E., Müller R. D., Chandra R. 2022. A review of machine learning in processing remote sensing data for mineral exploration. *Remote Sensing of Environment*. 268. doi: https://doi.org/10.1016/j.rse.2021.112750.

[19] Behera S., Panigrahi M. K. 2022. Gold prospectivity mapping and exploration targeting in Hutti-Maski schist belt, India: Synergistic application of Weights-of-Evidence (WOE), Fuzzy Logic (FL) and hybrid (WOE-FL) models. *Journal of Geochemical Exploration*. 235. doi: https://doi.org/10.1016/j.gexplo.2022.106963.

[20] Zhang S. E., Lawley C. J. M., Bourdeau J. E., Nwaila G. T., Ghorbani Y. 2024. Workflow-induced uncertainty in data-driven mineral prospectivity mapping. *Natural Resources Research*. 33: 995–1023. doi: https://doi.org/10.1007/s11053-024-10322-8.

[21] Zuo R., Kreuzer O. P., Wang J., Xiong Y., Zhang Z., Wang Z. 2021. Uncertainties in GIS-Based Mineral Prospectivity Mapping: Key Types, Potential Impacts and Possible Solutions. *Natural Resources Research*. 30: 3059–3079. doi: https://doi.org/10.1007/s11053-021-09871-z.

[22] Parsa M., Cumani R. 2025. Class label representativeness in machine learning-based mineral prospectivity mapping. *Natural Resources Research*. 34: 1901–1925. doi: https://doi.org/10.1007/s11053-025-10468-z.

[23] Ribeiro B. O. L., Barbuena D., de Melo G. H. C., Motta J. G., Marques E. D., Marinho M. S. 2024. How do non-deposit sites influence the performance of machine learning-based gold prospectivity mapping: A study case in the Pitangui Greenstone Belt, Brazil. *Journal of Geochemical Exploration*. 264. doi: https://doi.org/10.1016/j.gexplo.2024.107543.

[24] Lu M., Zhong L., He W. [et al.] 2026. Explainable Machine Learning in Mineral Prospectivity Mapping: A Critical Review of Methods, Geological Knowledge Embedding, Validation, and Future Directions. *Minerals*. 16(10). doi: https://doi.org/10.3390/min16101003.

УДК 519.63

ПФАФФИАНОВА СТРУКТУРА И СПЕКТРАЛЬНАЯ ДИНАМИКА ДИСКРЕТНОГО ОПЕРАТОРА ЛОТКИ–ВОЛЬТЕРРЫ: ПОДХОД К ИНТЕГРАЦИИ ГЕОЛОГИЧЕСКИХ ДАННЫХ

[1,2*] ***Эшмаматова Д.Б.,*** [1] ***Солижанова К.А.***

*24dil@mail.ru

[1]Ташкентский государственный транспортный университет, Ташкент, Узбекистан;

[2]Институт математики имени В.И. Романовского Академии наук Республики Узбекистан, Ташкент, Узбекистан

В статье исследуется связь между пфаффиановыми инвариантами, геометрией неподвижных точек и локальной спектральной динамикой дискретного операто-

ра Лотки–Вольтерры на четырёхмерном симплексе. Для турнира взаимодействий, содержащего четыре циклические тройки, единственные внутренние неподвижные точки соответствующих инвариантных двумерных граней образуют вершины карты неподвижных точек. На основе ранее установленного критерия ориентации и выбранного соглашения о знаках циклическая конфигурация этой карты характеризуется главными пфаффиановыми инвариантами четвёртого порядка. При положительности всех компонент пфаффианова вектора внутренняя неподвижная точка явно строится посредством нормированных отношений пфаффианов. Характеристический многочлен матрицы Якоби в этой точке выражается через коэффициенты взаимодействия и те же инварианты. Доказывается инвариантность касательного пространства симплекса относительно матрицы Якоби. Спектр её ограничения на это пространство состоит из двух пар комплексно-сопряжённых собственных значений с модулями больше единицы, что устанавливает локально отталкивающую динамику с колебательными компонентами. Полученные результаты объединяют геометрию неподвижных точек и локальное спектральное поведение в рамках единого алгебраического подхода и дают явные формулы, пригодные для вычислительного анализа. Также предлагается математическая интерпретация интеграции пяти групп геологических данных. Расстояния до конфигураций неподвижных точек и показатели отклика на взаимодействия вводятся как характеристики состава данных и взаимодействий между их группами. Их потенциальное использование для оценки перспективности на золото требует калибровки по данным геологоразведочных наблюдений и независимой эмпирической проверки.

Ключевые слова: дискретный оператор Лотки–Вольтерры, пфаффианов инвариант, карта неподвижных точек, внутренняя неподвижная точка, локальный спектр, оценка перспективности на золото

Цитирование: *Эшмаматова Д.Б., Солижанова К.А.* Пфаффианова структура и спектральная динамика дискретного оператора Лотки–Вольтерры: подход к интеграции геологических данных // Проблемы вычислительной и прикладной математики. – 2026. – № 5(76). – С. 95-118.

DOI: 10.71310/pcam.5_76.2026.07

№ 5(76) 2026

ISSN 2181-8460

HISOBLASH VA AMALIY MATEMATIKA MUAMMOLARI

ПРОБЛЕМЫ ВЫЧИСЛИТЕЛЬНОЙ И ПРИКЛАДНОЙ МАТЕМАТИКИ

PROBLEMS OF COMPUTATIONAL AND APPLIED MATHEMATICS

AiRI
RAQAMLI TEXNOLOGIYALAR VA SUN'IY INTELLEKTNI RIVOJLANTIRISH ILMIY-TADQIQOT INSTITUTI

ПРОБЛЕМЫ ВЫЧИСЛИТЕЛЬНОЙ И ПРИКЛАДНОЙ МАТЕМАТИКИ

№ 5(76) 2026

Журнал основан в 2015 году.
Издается 6 раз в год.

Учредитель:
Научно-исследовательский институт развития цифровых технологий и искусственного интеллекта.

Главный редактор:
Равшанов Н.

Заместители главного редактора:
Арипов М.М., Шадиметов Х.М., Ахмедов Д.Д.

Ответственный секретарь:
Убайдуллаев М.Ш.

Редакционный совет:
Азамов А.А., Алоев Р.Д., Амиргалиев Е.Н. (Казахстан), Арушанов М.Л., Абдуллозода С.Ф. (Таджикистан), Боборахимов Б.И., Бурнашев В.Ф., Джумаёзов У.З., Загребина С.А. (Россия), Задорин А.И. (Россия), Игнатьев Н.А., Ильин В.П. (Россия), Иманкулов Т.С. (Казахстан), Исмагилов И.И. (Россия), Кабанихин С.И. (Россия), Курбонов Н.М., Маматов Н.С., Мирзаев Н.М., Мурадов Ф.А., Назирова Э.Ш., Нормуродов Ч.Б., Нуралиев Ф.А., Нуралиев Ф.М., Опанасенко В.Н. (Украина), Расулмухамедов М.М., Садуллаева Ш.А., Старовойтов В.В. (Беларусь), Хаётов А.Р., Халджигитов А., Хамдамов Р.Х., Хужаев И.К., Хужаеров Б.Х., Эшмаматова Д.Б., Дустмуродова Ш.Ж., Чье Ен Ун (Россия), Шабозов М.Ш. (Таджикистан), Dimov I. (Болгария), Li Y. (США), Mascagni M. (США), Min A. (Германия), Singh M. (Южная Корея).

Журнал зарегистрирован в Агентстве информации и массовых коммуникаций при Администрации Президента Республики Узбекистан.
Свидетельство №0856 от 5 августа 2015 года.

ISSN 2181-8460, eISSN 2181-046X

При перепечатке материалов ссылка на журнал обязательна.
За точность фактов и достоверность информации ответственность несут авторы.

Адрес редакции:
100125, г. Ташкент, м-в. Буз-2, 17А.
Тел.: +(998) 71 263-41-98.
Э-почта: journals@airi.uz.
Веб-сайт: https://journals.airi.uz.

Дизайн и вёрстка:
Шарипов Х.Д.

Отпечатано в типографии НИИ РЦТИИ.
Подписано в печать 28.10.2026 г.
Формат 60x84 1/8. Заказ № 6. Тираж 100 экз.

PROBLEMS OF COMPUTATIONAL AND APPLIED MATHEMATICS

No. 5(76) 2026

The journal was established in 2015.
6 issues are published per year.

Founder:
Digital Technologies and Artificial Intelligence Development Research Institute.

Editor-in-Chief:
Ravshanov N.

Deputy Editors:
Aripov M.M., Shadimetov Kh.M., Akhmedov D.D.

Executive Secretary:
Ubaydullaev M.Sh.

Editorial Council:
Azamov A.A., Aloev R.D., Amirgaliev E.N. (Kazakhstan), Arushanov M.L., Abdullozoda S.F. (Tajikistan), Boborakhimov B.I., Burnashev V.F., Djumayozov U.Z., Zagrebina S.A. (Russia), Zadorin A.I. (Russia), Ignatiev N.A., Ilyin V.P. (Russia), Imankulov T.S. (Kazakhstan), Ismagilov I.I. (Russia), Kabanikhin S.I. (Russia), Kurbonov N.M., Mamatov N.S., Mirzaev N.M., Muradov F.A., Nazirova E.Sh., Normurodov Ch.B., Nuraliev F.A., Nuraliev F.M., Opanasenko V.N. (Ukraine), Sadullaeva Sh.A., Starovoitov V.V. (Belarus), Khayotov A.R., Khaldjigitov A., Khamdamov R.Kh., Khujaev I.K., Khujayorov B.Kh., Eshmamatova D.B., Dustmurodova Sh.J., Chye En Un (Russia), Shabozov M.Sh. (Tajikistan), Dimov I. (Bulgaria), Li Y. (USA), Mascagni M. (USA), Min A. (Germany), Singh M. (South Korea).

The journal is registered by Agency of Information and Mass Communications under the Administration of the President of the Republic of Uzbekistan.
Certificate of Registration No. 0856 of 5 August 2015.

ISSN 2181-8460, eISSN 2181-046X

At a reprint of materials the reference to the journal is obligatory.
Authors are responsible for the accuracy of the facts and reliability of the information.

Address:
100125, Tashkent, Buz-2, 17A.
Tel.: +(998) 71 263-41-98.
E-mail: journals@airi.uz.
Web-site: https://journals.airi.uz.

Layout design:
Sharipov Kh.D.

DTAIRI printing office.
Signed for print 28.10.2026
Format 60x84 1/8. Order No. 6. Print run of 100 copies.

Содержание

Расулов А.С., Раимова Г.М., Рахматов М.Й.
Метод Монте-Карло для решения нелинейного кинетического уравнения Больцмана 8

Эшкулов М.У., Хамдамов Р.Х.
Многокритериальная оптимизация системы подъёма воды с использованием солнечных фотоэлектрических панелей 22

Абдуллаев К.Д.
Принцип разделения классов и зависимость результатов кластеризации от меры расстояния 33

Рамазонов Ш.Ш.
Селекция объектов по отношениям с ближайшими объектами противоположного класса и сохранение локальной структуры обучающей выборки . . 46

Исомиддинов А.И., Акбарова А.А., Акбаров Б.Х.
Марковская переключающаяся векторная авторегрессия для скрытых гликемических режимов в реальных данных самоконтроля диабета: оценка на отложенной выборке 60

Ким К.К.
Сравнительный анализ XAI-подходов для обнаружения синтетической речи 72

Эшмаматова Д.Б., Солижанова К.А.
Пфаффианова структура и спектральная динамика дискретного оператора Лотки–Вольтерры: подход к интеграции геологических данных 95

Джумаёзов У.З., Абдирахмонова М.Н., Усмонов Л.С.
Численное решение трёхмерной связанной динамической задачи термоупругости в деформациях 119

Бакаев И.И., Ахмеджанова Д.А.
α-справедливая оптимизационная модель и численные алгоритмы выбора общей лексической нормы тюркских языков 137

Равшанов Н., Камолиддинова Ф., Lu Y.
Моделирование переноса и диффузии загрязняющих веществ в пограничном слое атмосферы с учётом орографии местности и метеорологических факторов 148

Contents

Rasulov A.S., Raimova G.M., Rakhmatov M.Y.
Monte Carlo solution of the nonlinear kinetic Boltzmann equation 8
Eshkulov M.U., Khamdamov R.Kh.
Multi-criteria optimization of solar photovoltaic-based water lifting systems . . . 22
Abdullaev K.D.
The principle of class separation and the dependence of clustering results on the distance measure 33
Ramazonov Sh.Sh.
Instance selection based on nearest-enemy relations and preservation of the local structure of a training sample 46
Isomiddinov A.I., Akbarova A.A., Akbarov B.X.
Markov-switching vector autoregression for latent glycaemic regimes in real-world diabetes self-monitoring data: an out-of-sample evaluation 60
Kim K.K.
Comparative analysis of XAI approaches for synthetic speech detection 72
Eshmamatova D.B., Solijanova K.A.
Pfaffian structure and spectral dynamics of a discrete Lotka–Volterra operator: a framework for geological evidence integration 95
Djumayozov U.Z., Abdirakhmonova M.N., Usmonov L.S.
Numerical solution of a three-dimensional coupled dynamic thermoelasticity problem in terms of strains 119
Bakayev I.I., Akhmedjanova D.A.
An α-fair optimization model and numerical algorithms for selecting a common lexical norm of Turkic languages 137
Ravshanov N., Kamoliddinova F., Lu Y.
Modeling pollutant transport and diffusion in the atmospheric boundary layer considering terrain orography and meteorological factors 148